ResearchGate

See discussions, stats, and author profiles for this publication at: https://www.researchgate.net/publication/258684131

Exploring the Origin of Crystalline Lamella Twist in Semi-Rigid Chain Polymers: the Model of Keith and Padden revisited

ARTICLE *in* MACROMOLECULES · SEPTEMBER 2012

Impact Factor: 5.8 · DOI: 10.1021/ma301446t

CITATIONS
17

READS
18

6 AUTHORS, INCLUDING:

Martin Rosenthal
European Synchrotron Radiation Facility
25 PUBLICATIONS **176** CITATIONS
SEE PROFILE

G. Portale
European Synchrotron Radiation Facility
107 PUBLICATIONS **1,194** CITATIONS
SEE PROFILE

Ed Samulski
University of North Carolina at Chapel Hill
288 PUBLICATIONS **9,824** CITATIONS
SEE PROFILE

Dimitri Ivanov
Université de Haute-Alsace
140 PUBLICATIONS **2,119** CITATIONS
SEE PROFILE

Available from: Dimitri Ivanov
Retrieved on: 31 January 2016

Macromolecules

Article

pubs.acs.org/Macromolecules

Exploring the Origin of Crystalline Lamella Twist in Semi-Rigid Chain Polymers: the Model of Keith and Padden revisited

Martin Rosenthal,[†] Giuseppe Portale,[‡,§] Manfred Burghammer,[‡] Georg Bar,[⊥] Edward T. Samulski,[∥] and Dimitri A. Ivanov[†,*]

[†]Institut de Sciences des Matériaux de Mulhouse, CNRS LRC7228, 15 rue Jean Starcky, 68057 Mulhouse, France

[‡]European Synchrotron Radiation Facility (ESRF), 6 rue Jules Horowitz, 38043 Grenoble, France

[§]Netherlands Organization for Scientific Research (NWO), DUBBLE beamline at the ESRF, 6 rue Jules Horowitz, 38043 Grenoble, France

[⊥]Analytical Technology Center, Analytical Technologies, Dow Olefinverbund GmbH, 06258 Schkopau, Germany

[∥]Department of Chemistry, University of North Carolina, Chapel Hill, North Carolina 27599-3290, United States

ABSTRACT: The microstructure of banded spherulites of a typical semirigid-chain polymer, poly(trimethylene terephthalate), PTT, has been explored with microbeam X-ray diffraction. It is shown that during microbeam scans along the spherulite radius, different diffraction peaks exhibit oscillations with the same periodicity, which means that the lamellar twist is strictly uniform and regular. The twisted PTT crystals formed from the melt at 170 °C reveal a one-to-one correlation between the handedness and growth axis polarity. Thus, the lamellae are right-handed for the growth along the negative growth direction (−**a**) while they are left-handed for the positive growth direction (+**a**). This is in line with predictions of the KP-model, although the original model cannot explain why, for example left-handed crystals have to grow along (−**a**). The direction of the chain tilt in the lamellar crystal correlates with the lamellar handedness as postulated by the KP-model. However, the measured chain tilt in the crystal (4°) is too faint to be the primary source of the surface stresses required for twisted lamellar growth.

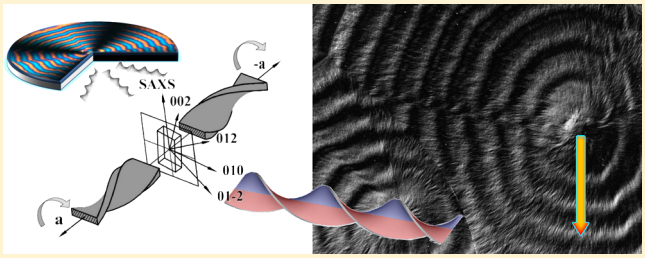

INTRODUCTION

The structure of banded polymer spherulites has been one of the most debated problems in polymer physics over the last decades. The major contributions to this field have been made by Keith and Padden[1−4] and later on by Lotz and Cheng[5] and Toda.[6,7] Spectacular patterns of concentric extinction rings of banded spherulites, as revealed by polarized optical micrographs (cf. Figure 1, top), are conventionally interpreted as a result of a highly correlated twisted growth of lamellar crystals.[3,8,9] Since the initial discovery of this morphological feature, lamellar twist has been identified as a phenomenon occurring at the crystal growth front. It has been also recognized as a property of individual lamellar crystals or lamellar crystal stacks. Two main models of the origin of this spectacular morphology will be referred to here. The first one explains the lamellar twist as a consequence of cumulative reorientation of lamellae via successive isochiral screw dislocations, as suggested by Basset and Hodge[10−13] and later on elaborated further by Toda.[14] In the second model, described in the seminal work of Keith and Padden,[15−17] it is the unbalanced stresses at the lamellar surface due to differential congestion of the chain folds that are considered to be the main cause of lamellar twist.

In the model of Keith and Padden (KP-model) the chirality of lamellar crystals formed from achiral polymers such as polyethylene (PE) was posited to result from a tilt of the stems relative to the basal lamella plane. The chain tilt was suggested to bring about differential congestion of the chain folds on the lamella surfaces. The resulting positive (σ^+) and negative surface stresses (σ^-) induce twisting of the planar lamella crystal to alleviate stress. In Figure 1 (middle), we depict a lamellar crystal growing along its long axis |**a**| by condensing rows of folded chain stems into successive facets normal, or inclined at some angle, to |**a**| (with propagation rate ***g***) accreting fold surface on either side of the lamella and giving the overall macroscopically observable growth rate ***G***. If one were to cut the crystalline lamella along |**a**|, the resulting strips would bend either up or down, depending on the sign of the surface stresses. Hence, the contiguous lamella reduces its mechanical energy by adopting a twisted helicoidal shape (cf. Figure 1 bottom). If one assumes that the distribution of surface stresses is indeed the one implied by the KP-model, it is possible to show that the handedness of the lamella helicoid is directly

Received: July 12, 2012
Revised: August 11, 2012
Published: September 7, 2012

ACS Publications © 2012 American Chemical Society

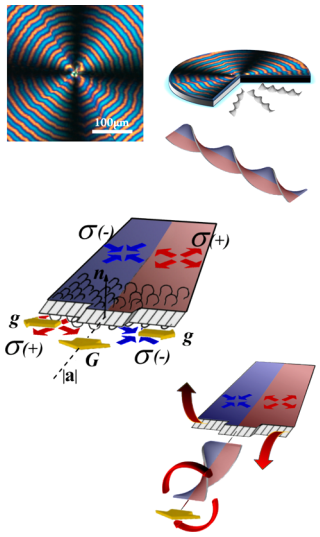

Figure 1. Polarized optical micrograph of a banded spherulite of poly(trimethylene terephthalate) (top left). Schematic depicting a quasi-2D spherulite with bands due to synchronous helicoidal twist of the crystalline lamellae (top right). The model of a twisted crystalline lamella according to Keith and Padden,[15] in which the lamellar twist is generated by unbalanced surface stresses having different signs on opposite fold surfaces and on both longitudinal halves of the lamella (bottom).

correlated with the polarity of the crystal growth direction. This follows from the fact that the pattern of stresses generated on the lamellar surface possesses mirror plane symmetry about a plane perpendicular to the long axis of the lamella and passing through the spherulite center. The mirror-plane operation obviously inverts the sense of twist of a chiral object so that a lamella growing radially out from the spherulitic center will necessary have different handedness in the opposing hemispheres of the spherulite.

Here it is important to stress a nontrivial difference between a twisted lamellar crystal and a simple screw. For the case of a screw, its handedness obviously does not change when the screw is placed upside down or observed from different ends. The situation with a lamellar crystal is completely different. The handedness of the lamella does depend on the conditions and local environment at the crystal growth front, i.e., during its formation. Thus, if the stress distribution gives rise to a right-handed twist at one tip of the growing crystal, the mirrored stresses will necessarily produce a left-hand twist at the opposite tip of the crystal. Therefore, the polarity of the growth axis has a crucial impact on the lamella handedness, and inversion of the growth direction will affect the lamellar handedness. Importantly, in the framework of the KP-model, these considerations are independent of the particular symmetry of the unit cell. Moreover, the KP-model postulates that there is a one-to-one correlation between the lamella handedness and the direction of the chain tilt, e.g., left-handed lamellae are formed when the chains are tilted to the left with respect to the lamellar normal ***n*** when looking in the growth direction (Figure 1, bottom) and vice versa.[18] Specifically, the authors say:[18] "Our presumption of greater congestion and larger stress in fold surfaces laid down at acute-angled edges of tilted growth faces was in the first instance dictated by empiricism, and the rationale we proposed was tentative". Therefore, to confirm the KP-model, one has to correlate the handedness of the lamellar helicoids not only with the direction of the chain tilt but also with the crystallographic growth axis polarity. But the determination of the latter is possible only for crystal lattices with low symmetry. For example, for polyethylene the discrimination between **+b** and **−b** axes from diffraction experiments alone is impossible.

In the past, the twisted lamellar morphologies were studied in much detail by electron microscopy on surfaces of chemically etched spherulites by Bassett and Olley,[19] by polarized optical microscopy equipped with electro-optical liquid crystal modulators,[20] or by surface-sensitive techniques such as atomic force microscopy (AFM).[21−24] The optical studies on spherulites of poly(3-hydroxyvalerate) allowed, for example, one to identify different sectors with right- or left-handed twist depending on the growth axis (in this case, **b** and **a**, respectively).[20] The AFM studies enabled in some cases time-resolved imaging of the lamellar growth, and provided a wealth of structural information as to the shape and spatial organization of the lamellar crystals. Despite extensive morphological studies performed on banded polymer spherulites, many important issues remain unsolved yet. It is, for example, still unclear what the exact shape of the twisted lamella is and whether it can be approximated by the classical helicoid with a uniform twist around its screw axis. To address this question, a detailed microstructural analysis of banded polymer spherulites in 3D is required, since the micrographs provided by conventional microscopy techniques are insufficient to visualize the 3D lamellar organization in such complex hierarchical structures.

Microbeam X-ray diffraction has been employed to address these problems since the beginning of 1960s.[25] More recently, this technique has gained importance due to its enhanced, and continuously improving, spatial resolution achieved on modern synchrotron-based microbeam setups.[26,27] X-ray microdiffraction is a rather unique structural analysis tool because it can assess the microstructure of samples, which are thick enough to exhibit spherulite banding, i.e., for polymer morphologies typical of the bulk. Such sample thicknesses are clearly out of reach for conventional selected-area electron diffraction (SAED). The information on the shape and structure of the twisted lamellar crystals is encoded in the microdiffraction pattern asymmetry and angular broadening (arcing) of reflections, as well as in the variation of the diffracted intensity as a function of radial distance. In the past, the angular broadening of the off- meridional diffraction peaks in the SAED patterns has been used to analyze the shape of isolated helicoidal ribbons of a main-chain chiral polyester.[28] On the basis of this data, the authors deduced the twist angles along both axes, i.e., the long and short axes, of the helicoid. Some analytical and computational approaches toward the lamellar shape analysis based on microfocus X-ray diffractograms have been developed by one of the authors[29−31] and applied to the case of lamellar twist in poly(trimethylene terephthalate).[32]

In our previous work, the technique of microbeam X-ray diffraction applied to banded spherulites of high-density PE allowed testing of the validity of the KP-model by correlating the direction of the chain tilt with the handedness of the twisted lamellae.[33] When looking along the fast crystal growth axis the tilt of the crystalline stems to the right from the lamellar normal results in a right-handed twist of the growing lamella and vice versa, i.e. according to the predictions of the KP-model. Thus, it can be shown that during crystallization the chain tilt in the lamella imparts chirality to the otherwise achiral chain of PE. Although the sense of lamellar twist in PE is found

dx.doi.org/10.1021/ma301446t | *Macromolecules* 2012, 45, 7454−7460

to correlate with the direction of the crystalline stem as depicted in Figure 1 (bottom), its correlation with the growth axis polarity cannot be established from the X-ray data alone. Here, only indirect evidence for the correlation between the lamellar twist sense and growth axis polarity was found. This comes from the fact that, when scanning with the X-ray microbeam along the spherulite radius, the handedness of the lamella was found to invert in the spherulite center, which may be a consequence of the growth axis polarity inversion in the type II spherulites. However to our knowledge, the challenge of directly correlating the growth axis polarity with the lamella handedness has never been addressed for polymer spherulites to date.

EXPERIMENTAL SECTION

Poly(trimethylene terephthalate) (PTT) from Corterra (CP 509200) with molecular M_w = 35200 g·mol^{-1} and polydispersity of 2.0 was used in the study. Free-standing films of approximately 30 μm thickness were prepared by melt crystallization at 170 °C between cover glass slides followed by floating the films off on water after immersion in 1% HF for 24 h. For the structural analysis, the PTT unit cell parameters were taken from the literature.[34]

Microbeam X-ray diffraction experiments were conducted at the ID13 beamline of the European Synchrotron Radiation Facility (ESRF) (Grenoble, France). The measurements were performed in transmission with the sample surface normal to the X-ray beam using the crossed-Fresnel optics and the wavelength of 1.0 Å. A Frelon CCD was employed to record the 2D X-ray patterns. The size of the monochromatic X-ray beam at the focus point was 500 nm along both axes. The norm of the scattering vector **s** ($s = 2\sin(\theta)/\lambda$) was calibrated using several reflections of corundum. The region of interest was selected with an on-axis optical microscope operated in reflection. Further refinement of the beam position on the sample was carried out using the azimuthal angles of the diffraction peaks on 2D diffractograms. During data collection the sample was scanned by means of an x-y gantry using steps of 1 μm along the radial direction of the spherulites. The data reduction and analysis including geometrical and background correction, visualization and the radial as well as the azimuthal integration of the 2D diffractograms were performed using home-build routines within the IgorPro software package.

RESULTS AND DISCUSSION

Figure 2 (top right) displays a microfocus X-ray diffraction pattern, which was obtained by summing up several tens of frames acquired during a microbeam scan performed along the radius of a banded spherulite of PTT shown with the yellow arrow (cf. Figure 2, top left).

Upon indexing the peaks on the diffractogram it can be seen that the 0*kl* reflections are all positioned on the equatorial direction, which means that the crystal growth direction (i.e., the meridian of the diffractogram) corresponds to the *a*-parameter of the PTT unit cell. This is in agreement with previous studies of PTT performed using SAED.[35] Furthermore, the averaged diffractogram (Figure 2, top right) suggests a uniaxial symmetry as it is observed for example for drawn fibers. However, in this case the rotation axis does not correspond to the chain axis of the polymer but to the fast crystal growth axis. The corresponding molecular model showing the orientation of the unit cell with respect to the uniaxial symmetry axis is given in Figure 2 (bottom right). Importantly, the WAXS patterns also allow observing the SAXS signal resulting from the PTT lamellar stacks in the edge-on orientation. This is explained by a relatively small long period of the semicrystalline structure of PTT (i.e., less than 10 nm). The SAXS signal provides important additional information as to

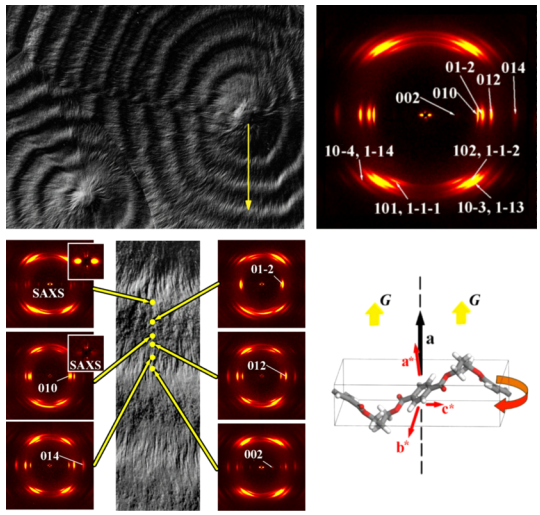

Figure 2. Confocal scanning optical micrograph of a PTT free-standing film, as used for the microfocus X-ray experiments (top left) shows the banded spherulitic texture. The direction of scanning is indicated by the yellow arrow. Average X-ray diffraction pattern obtained by summing up over the whole radial scan (top right). Set of X-ray diffraction patterns corresponding to the maximum intensity of the indexed reflections as a function of radial position relative to the banded morphology shown in the gray insert (bottom left). The radial direction of the spherulite is vertical. The fiber symmetry of the pattern is due to rotation of the growing crystal around its **a**-axis as shown in the sketch (bottom right).

the orientation of the PTT chains with respect to the normal to the lamella basal plane.

The hypothesis that the local structure of banded spherulites of PTT resembles more a single-crystal-like texture than the structure of polycrystalline material is supported by the X-ray microbeam patterns given in Figure 2 (bottom left). The set of X-ray diffraction patterns is representative of situations where the indicated reflections reach their maximal intensity in the course of the radial scan. In the top pattern the SAXS signal has its maximum while the 010 reflection is almost undetectable. Approximately halfway between the two successive regions with edge-on oriented crystalline lamellae the 010 reflection reaches its maximum, while the SAXS signal completely disappears. This corresponds to the flat-on orientation of the PTT crystals. In general, the periodic appearing and disappearing of the diffractions peaks reflects the periodic change in the crystal orientation as a function of the radial distance, while in none of the patterns all reflections coexist. Among the observed reflections, the most intense are 010, 01$\bar{2}$, and 012 equatorial reflections, while the doublets 101/1$\bar{1}\bar{1}$, 102/1$\bar{1}$2, 10$\bar{3}$/1$\bar{1}$3 and 10$\bar{4}$/1$\bar{1}$4 are located on the first layer line. The calculated and measured *d*-spacings are summarized in Table 1. In addition, for each reflection we computed the azimuthal angle ρ, i.e., the angle between the arbitrary reciprocal-space vector *hkl* and the meridional **a**-axis, and the fiber angle φ, which is defined as the angle between the projections of the arbitrary reciprocal-space vector and the 010 vector in the plane normal to **a** (cf. Figure 3).

Despite the fact that the unit cell of PTT is triclinic, the recorded microfocus X-ray patterns clearly reveal layer lines (the lattice is in fact only slightly triclinic with angle β close to 90°). Thus, the first layer line exhibits intense reflections grouped in doublets having the characteristic indices *h*0*l*, *h*1$\bar{1}$*l*. The doublet peaks completely merge on one-dimensional

dx.doi.org/10.1021/ma301446t | Macromolecules 2012, 45, 7454−7460

Table 1. Experimental and Calculated *d*-Spacings, Azimuthal (ρ), and Sagittal (φ) Angles for the Most Intense Reflections Shown in Figure 2

h	*k*	*l*	d_{hkl}, Å	d_{hkl}*, Å	ρ, deg	φ, deg	φ*, deg
0	0	2	9.208	9.187	90.0	81.3	82
0	1	0	5.692	5.714	90.0	ref	ref
0	1	−2	5.185	5.235	90.0	33.9	35
0	1	2	4.558	4.545	90.0	28.8	29
0	1	4	3.352	3.437	90.0	45.1	47
SAXS			–	34	90.0	–	84
1	0	1	4.170	4.115	27.2	31.2	33} doublet
1	−1	−1	4.082		27.5	153.6	
1	0	2	3.838	3.802	35.2	46.9	48} doublet
1	−1	−2	3.778		35.0	136.6	
1	0	−3	3.652	3.610	37.9	69.5	67} doublet
1	−1	3	3.563		39.4	111.4	
1	0	−4	3.260	3.245	45.1	76.7	78} doublet
1	−1	4	3.191		46.3	104.3	

*Experimentally measured.

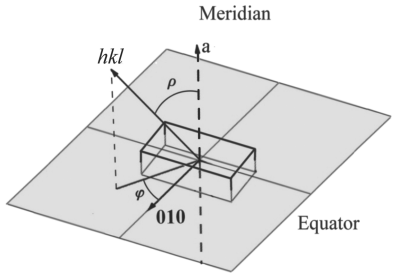

Figure 3. Schematic drawing showing an arbitrary reciprocal-space vector *hkl*, its azimuthal angle ρ with respect to the meridian of the X-ray pattern (**a**-vector) and the fiber angle φ between the projections of the *hkl* vector on a plane normal to **a** and 010 vector.

diffraction curves, which can be accounted for by the fact that their *d*-spacings are very close. The azimuthal angles ρ of the doublet peaks are identical while their corresponding fiber angles φ are approximately supplementary, i.e., giving 180° when added up. This means that these reciprocal-space vectors are almost lying in one plane together with the rotation axis **a** as depicted in Figure 4. This fact adds an additional quasi-symmetry element to the low-symmetry P-1 unit cell of PTT. Therefore, in further analysis, the pairs of the *h*0*l*, $h\bar{1}\bar{l}$

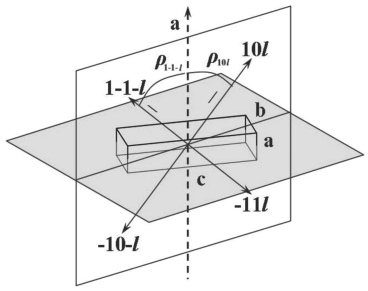

Figure 4. Schematic drawing exemplifying the position of off-meridional doublet peaks of the first layer line of the PTT X-ray patterns. The indicated reciprocal-space vectors and the **a**-vector are approximately located in one plane. The azimuthal angle ρ is almost identical for vectors *h*0*l* and $h\bar{1}\bar{l}$.

reflections can be approximated to the phenomenon of multiplicity pertinent to higher-symmetry lattices.

The normalized intensity of the most intense reflections of the equator and first layer line are given in Figure 5. All curves

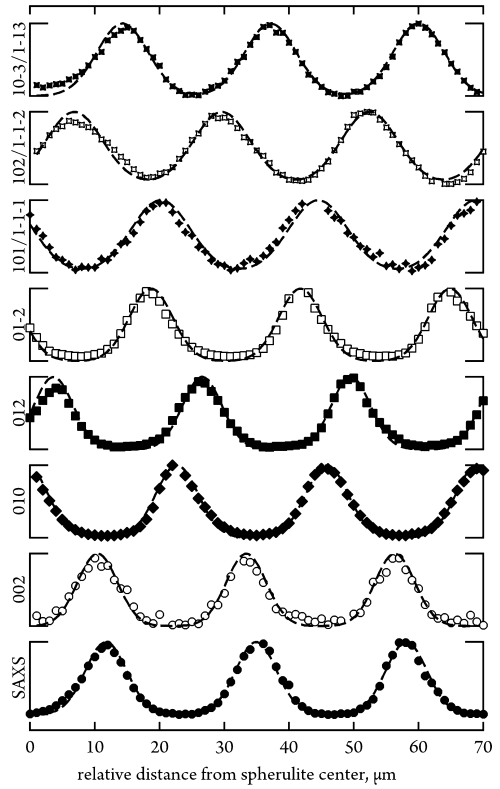

Figure 5. One-dimensional profiles of the diffracted intensity of the most intense equatorial and first-layer-line reflections as a function of distance from the spherulite center. The characteristic periodic behavior results from rotation of the reciprocal-space vectors moving in and out of the reflection conditions.

reveal a clear oscillation behavior with the same periodicity reaching their maxima at different radial positions. The periodic oscillation of the diffracted intensity is due to rotation of the reciprocal-space vectors entering and exiting the reflection conditions while scanning the spherulite radially.

From Fourier analysis of the one-dimensional intensity profiles given in Figure 5, one finds the periodicity of 23.25 μm, which corresponds to half period of the lamellar twist. This value is in excellent agreement with the bandwidth measured by optical microscopy. The occurrences of the main diffraction peaks maxima along the radial scan are shown in Figure 6. The φ-values of the peaks merge on one line as a function of the radial peaks position, which signifies that the lamellar twisting is strictly uniform and regular. This observation is more compatible with the model explaining the twist as a result of unbalanced surface stresses rather than from giant screw dislocations. It is noteworthy that previous studies on thin films of PTT with SAED indicate that lamellar twist is likely to be discontinuous because several preferred orientations of the crystals were identified.[36] Since this situation is not characteristic of the bulk structure, such an effect may be caused by spatial confinement of the lamellae in thin PTT films amenable to the electron diffraction technique.

Taking into account the fact that the twist is regular and continuous, it is possible to calculate the phase shift of the

dx.doi.org/10.1021/ma301446t | *Macromolecules* 2012, 45, 7454−7460

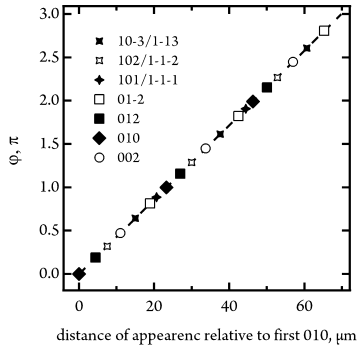

Figure 6. Values of the fiber angle φ pertinent to several intense reflections. These show a linear behavior as a function of the radial distance. This observation provides support to the model of continuously rotating crystal and thus to a regular and uniform twist of the growing lamellae.

different reflections using the twisting period and radial distance of the particular reflection. The phase shifts of the main equatorial reflections as a function of the crystallographic angle relative to the 010 reflection are summarized in Figure 7 (left).

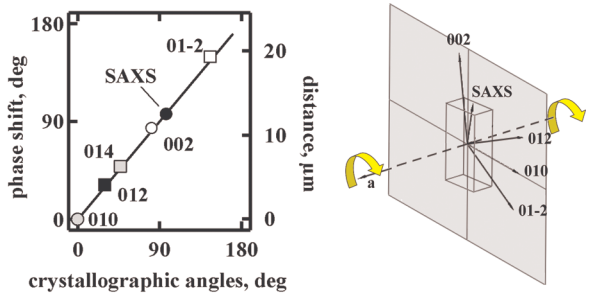

Figure 7. The phase shift of the strongest equatorial reflections as a function of angle φ of the corresponding reciprocal-space vectors with respect to the 010 peak (left). Sketch illustrating the PTT crystal rotation about the **a**-axis (right). The equatorial 0*kl* vectors rotate in the **b***c*-plane. The sense of the crystal rotation is indicated by the yellow arrows.

The linear behavior ($y = x$) observed in Figure 7 (left) shows that the lamellar stacks have a single-crystal-like, local-scale texture, and uniformly rotate around the growth axis **a**. This is similar to the conclusion obtained for the microstructure of banded spherulites of PE.[33] However, in the case of PTT, due to the triclinic nature of the unit cell, it is possible to derive the sense of the crystal rotation directly from the sequence of appearance of equatorial peaks. Indeed, for example the sequence of peak appearances such as $01\bar{2} \rightarrow 010 \rightarrow 012$ will correspond to the clockwise rotation of the crystal when looking along the -**a**-direction (cf. Figure 7, right). Since the equatorial reflections rotate in the **b***c*-plane (gray parallelogram in the same figure), which is normal to the **a**-vector, the handedness of the growing lamellar stacks should be linked to the growth axis polarity, as it can be deduced from the original assumptions of Keith and Padden.[37] Therefore, the case of PTT provides an interesting opportunity to verify the KP-model by correlating the growth-axis polarity to the lamellar stack handedness, which can be determined from microfocus X-ray diffraction experiments using the finite curvature of the Ewald sphere.[32,33]

Figure 8 depicts the Ewald sphere construction showing the conditions for observation of an arbitrary diffraction peak. To

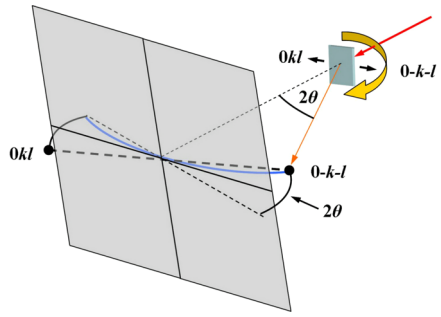

Figure 8. Schematic drawing depicting the Ewald sphere, which allows determining the handedness of the lamellar helicoid from the positions of the maximum intensity of symmetric reflections, e.g., 0*kl* and $0\bar{k}\bar{l}$. The equatorial section of the Ewald sphere is indicated by the blue arc. The position of the reciprocal space vector on the Polanyi sphere[38,39] is given by the black spheres. The rotation direction of the sample indicated in light blue is shown by the yellow arrow.

be observed experimentally, the corresponding reciprocal space vector should make an angle θ (Bragg angle) with the plane perpendicular to the incident X-ray beam direction. During twisting of the crystalline lamellar ribbon, the symmetric diffraction peaks (i.e., 0*kl* and 0-*k*-*l*) will enter the reflection conditions at different moments.

In particular, for a right-handed helicoid oriented vertically, which is scanned in the downward direction, the peak on the right side of the detector (if one looks upstream at the X-ray beam) should appear before its symmetric counterpart on the left side of the detector. The angular distance between the maxima of the two peaks should equal twice the Bragg angle, i.e., 2θ. Thus, the finite curvature of the Ewald sphere provides a delicate way to discriminate the lamellar helicoids according to their handedness.

Figure 9 shows the peak intensity and azimuthal position of the equatorial 010 reflection as a function of the radial distance from the spherulite center corresponding to the scan shown in

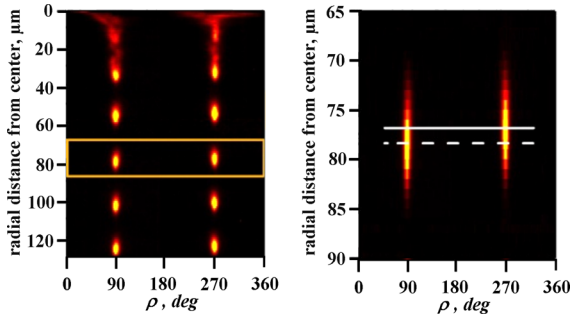

Figure 9. Intensity and azimuthal position of the equatorial 010 reflection as a function of the radial distance from the spherulite center (left). The reflection on the right side of the detector (i.e., at an azimuthal angle ρ of 270°) appears slightly before the left-side reflection (i.e., at ρ equal 90°). This indicates a right-handed rotation of the crystal about the **a**-axis (cf. Figure 7) when the lamella grows downward (right). The relative phase shift in the peak appearance corresponds to twice the Bragg angle of the corresponding peak. The diffuse and irregular appearance close to the center of the spherulite is due to inclination of the crystal growth direction with respect to the film surface occurring in this region because of finite film thickness.

dx.doi.org/10.1021/ma301446t | *Macromolecules* 2012, 45, 7454−7460

Figure 5. Besides the oscillation of the reflection intensity, one can see that the reflection is positioned strictly on the equatorial direction at 90° and 270° if one assigns angle of 0° to the meridian. Here, the reflection at 90° corresponds to the peak showing up on the left side of the detector when looking upstream the X-ray beam while the right-side reflection appears at 270° (cf. Figure 2). The equatorial peaks do not show any wagging about the equator indicating that, within the precision of the measurement, the lamellar shape is not helical but helicoidal.

By examining the appearance of the left- and right-side reflections in more detail (cf. Figure 9, right) it can be seen that on the right side of the detector the peak shows up slightly before its left counterpart, having a difference of ca. 1.5 μm. When recalculated in terms of the phase angle (app. 10°), this difference corresponds to twice the Bragg-angle of the 010 reflection for the given wavelength. This means that the studied helicoid is right-handed. Considered together with the rotation sense of the crystal it follows then that the growth axis polarity is negative, i.e., −**a**. The corresponding vector model is depicted in Figure 10.

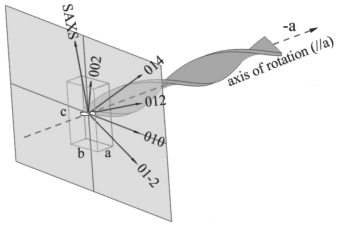

Figure 10. Vector model of a rotating PTT crystal, which grows in the −**a**-direction.

To check whether the negative growth axis polarity is correlated to the right sense of rotation of the crystal, microfocus scans were performed on tens of PTT spherulites. Remarkably, it was found that, when scanning the spherulite from its center outward, the diffraction peaks always reveal the same sequence of appearance, i.e., $01\bar{2}$ peak is followed by 010 and then by the 012 peak. Thus, the crystal rotation direction within the **b***c* plane is always identical, independently of whether the crystal growth occurs along **a** or −**a** direction. Most importantly, we found that there is indeed a one-to-one correlation between the polarity of the crystal growth axis and the handedness of the lamella helicoid, that is the lamellae are right-handed for the growth along the negative growth direction (−**a**) while they are always left-handed for the positive direction. A model summarizing these observations is depicted in Figure 11. This observation is consonant with predictions of the KP-model, although the model cannot explain why, for example, left-handed crystals have to grow along −**a** and not along **a**.

Now we turn to consideration of the other premise of the KP-model, i.e., the statement that chain tilt to the right of the lamella normal induces right-handed lamellar twist when seen in the direction of the lamellar growth axis and vice versa.[18] For this purpose, it is necessary to analyze the phase angle of the SAXS signal with respect to other equatorial reflections.

Figure 7 (left) shows that the SAXS signal does not appear simultaneously with the 002 reflection indicating that the lamellar basal plane does not exactly correspond to the **ab**-plane of the crystal, as it was suggested by Ho,[35] but is instead

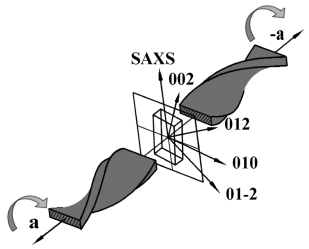

Figure 11. Schematic illustrating the reciprocal space vectors of the PTT unit cell rotating about the crystallographic *a*-axis, as shown with light gray arrows. All 0*kl* reflexes rotate in the plane perpendicular to **a**-vector. The sense of twist is right-handed for the growth along the negative growth direction (−**a**) while it is left-handed for the positive direction (**a**).

inclined in the plane perpendicular to **a**. Recalling that the angle between the **a** and **c** vectors is close to 90°, the chain tilt in the **a**-direction can be neglected. Using the positions of the strong equatorial reflections it is possible to derive the inclination of the unit cell in the plane perpendicular to **a** and thus the chain tilt in this direction.

The phase angle of the SAXS signal with respect to the 010 reflection is 84° (cf. Table 1), which corresponds to inclination of the **ab**-plane for about 12° in the positive **b**-direction. This means that the chain tilt is about 4° in this direction, as depicted in Figure 12. Therefore, the negative polarity of the

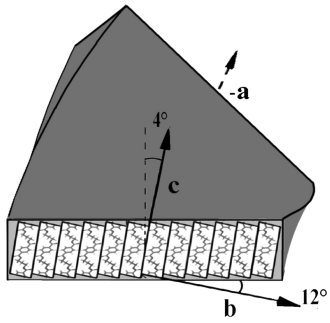

Figure 12. Orientation of the unit cell relative to the lamellar basal plane showing the inclination of the chain stems by about 4 degrees along **b*** and inclination of the **ab**-plane for about 12°.

growth axis correlates with right-handed twist of the lamella and corresponds to the chain tilt to the right from the lamella normal and vice versa (cf. Figures 11,12). It is noteworthy that the chain tilt has a unique direction across the whole lamellar stack, and the direction of the chain tilt is unequivocally determined by the crystallography of the PTT unit cell. In this sense, a lamellar stack in a melt-crystallized polymer is different, for example, from a crystal mat in which the stacked crystals can have different stem directions. Clearly, in a twisted lamellar stack of a melt-crystallized polymer the crystals with opposite stem orientation cannot coexist during growth because they will necessarily collide with each other due to the opposing twist sense.

The established correlations formally satisfy the premises of the KP-model. However, despite the agreement with the KP-model for the case of PTT, the value of the chain tilt of 4° does not appear to us to be sufficient for generation of the surface stresses required for twisted lamellar growth. For comparison, the chain tilt in melt-crystallized polyethylene[33] is as high as 35°. Therefore, further studies of the origin of lamella twist will

dx.doi.org/10.1021/ma301446t | *Macromolecules* 2012, 45, 7454−7460

be required to clarify whether or not the chain tilt alone is responsible for the formation of the banded spherulite morphology.

CONCLUSIONS

The use of microbeam X-ray diffraction for studies of the banded spherulite microstructure is discussed for the case of melt-crystallized poly(trimethylene terephthalate). It is shown that in the course of microbeam scans along the spherulite radius, the diffraction peaks exhibit oscillations with the same periodicity, which means that the lamellar twist is strictly uniform and regular. The latter observation is more compatible with the model explaining the twist as a result of unbalanced surface stresses than the giant screw dislocations.

On the basis of tens of micro beam X-ray diffraction scans across PTT spherulites, we conclude that the PTT crystals reveal a one-to-one correlation between the handedness and the growth axis polarity. Thus, the lamellae are right-handed for the growth along the negative growth direction (−**a**) while they are left-handed for the positive growth direction (**a**). This fact is a direct consequence of the KP-model predictions, which can be derived from the pattern of the surface stresses. However the model itself cannot explain why left-handed crystals have necessarily to grow along (−**a**) and not along (**a**). The observation that the direction of the chain tilt in the lamellar crystal correlates with the lamellar handedness is also consonant with the KP-model, namely that the lamellar twist is driven by surface stresses.[15,16] However, despite the formal agreement with the KP-model, the value of the chain tilt of 4° alone does not appear to us to be sufficient for generation of the surface stresses required for twisted lamellar growth. Therefore, further studies of twisted crystalline lamellae including determination of the growth axis polarity and the exact 3D-shape are needed to provide more insights into the nature of chirality of such supramolecular objects formed by achiral polymers.

AUTHOR INFORMATION

Corresponding Author

*E-mail: dimitri.ivanov@uha.fr.

Author Contributions

The manuscript was written through contributions of all authors. All authors have given approval to the final version of the manuscript.

Funding

Notes

The authors declare no competing financial interest.

ACKNOWLEDGMENTS

The financial support by the French Agence Nationale de la Recherche and German Research Foundation (ANR-DFG project “T2T”, MO 628/13-1) and IUPAC Project PAC-PAL-10-02-26 is gratefully acknowledged.

REFERENCES

(1) Keith, H. D.; Padden, F. J. *J. Polym. Sci.* **1958**, *31*, 415.
(2) Keith, H. D.; Padden, F. J. *J. Polym. Sci.* **1959**, *39*, 101.
(3) Keith, H. D.; Padden, F. J. *J. Polym. Sci.* **1959**, *39*, 123.
(4) Keith, H. D.; Padden, F. J. *J. Appl. Phys.* **1964**, *35*, 1286.
(5) Lotz, B.; Cheng, S. Z. D. *Polymer* **2005**, *46*, 577.
(6) Toda, A.; Okamura, M.; Taguchi, K.; Hikosaka, M.; Kajioka, H. *Macromolecules* **2008**, *41*, 2484.
(7) Toda, A.; Taguchi, K.; Kajioka, H. *Macromolecules* **2008**, *41*, 7505.
(8) Keller, A. *J. Polym. Sci.* **1959**, *39*, 151.
(9) Price, F. P. *J. Polym. Sci.* **1959**, *39*, 139.
(10) Bassett, D. C.; Hodge, A. M. *Polymer* **1978**, *19*, 469.
(11) Bassett, D. C.; Hodge, A. M.; Olley, R. H. *Faraday Discuss.* **1979**, *68*, 218.
(12) Bassett, D. C.; Hodge, A. M. *Proc. R. Soc. London A* **1981**, *377*, 61.
(13) Bassett, D. C. *J. Macromol. Sci.* **2003**, *B42*, 227.
(14) Toda, A.; Arita, T.; Hikosaka, M. *Polymer* **2001**, *42*, 2223.
(15) Keith, H. D.; Padden, F. J. *Polymer* **1984**, *25*, 28.
(16) Keith, H. D.; Padden, F. J.; Lotz, B. *Macromolecules* **1989**, *22*, 2230.
(17) Keith, H. D. *Polymer* **2001**, *42*, 9987.
(18) Keith, H. D.; Padden, F. J. *Macromolecules* **1996**, *29*, 7776.
(19) Bassett, D. C.; Olley, R. H. *Polymer* **1984**, *25*, 935.
(20) Ye, H.-M.; Xu, J.; Guo, B.-H.; Iwata, T. *Macromolecules* **2009**, *42*, 694.
(21) Ivanov, D. A.; Nysten, B.; Jonas, A. M. *Polymer* **1999**, *40*, 5899.
(22) Basire, C.; Ivanov, D. A. *Phys. Rev. Lett.* **2000**, *85*, 5587.
(23) Ivanov, D. A.; Amalou, Z.; Magonov, S. N. *Macromolecules* **2001**, *34*, 8944.
(24) Ivanov, D. A.; Bar, G.; Dosiere, M.; Koch, M. H. J. *Macromolecules* **2008**, *41*, 9224.
(25) Fujiwara, Y. *J. Appl. Polym. Sci.* **1960**, *10*, 10.
(26) Gazzano, M.; Focarete, M. L.; Riekel, C.; Ripamonti, A.; Scandola, M. *Macromol. Chem. Physic.* **2001**, *202*, 1405.
(27) Tanaka, T.; Fujita, M.; Takeuchi, A.; Suzuki, Y.; Uesugi, K.; Doi, Y.; Iwata, T. *Polymer* **2005**, *46*, 5673.
(28) Li, C. Y.; Cheng, S. Z. D.; Ge, J. J.; Bai, F.; Zhang, J. Z.; Mann, I. K.; Harris, F. W. *Phys. Rev. Lett.* **1999**, *83*, 4558.
(29) Luchnikov, V. A.; Ivanov, D. A. *J. Appl. Crystallogr.* **2009**, *42*, 673.
(30) Luchnikov, V. A.; Ivanov, D. A. *J. Appl. Crystallogr.* **2010**, *43*, 578.
(31) Luchnikov, V. A.; Anokhin, D. V.; Bar, G.; Cheng, S. Z. D.; Wang, C.-L.; Ivanov, D. A. *J. Appl. Crystallogr.* **2011**, *44*, 540.
(32) Rosenthal, M.; Anokhin, D. V.; Luchnikov, V. A.; Davies, R. J.; Riekel, C.; Burghammer, M.; Bar, G.; Ivanov, D. A. *IOP Conf. Ser.: Mater. Sci. Eng.* **2010**, *14*, 012014.
(33) Rosenthal, M.; Bar, G.; Burghammer, M.; Ivanov, D. A. *Angew. Chem., Int. Ed.* **2011**, *50*, 8881.
(34) Hall, I. H. The determination of the structures of aromatic polyesters from their wide-angle diffraction patterns. In *Structure of Crystalline Polymers*; Hall, I. H., Ed.; Elsevier Applied Science Publ.: London and New York, 1984; pp 39−78.
(35) Ho, R. M.; Ke, K. Z.; Chen, M. *Macromolecules* **2000**, *33*, 7529.
(36) Wang, B. J.; Li, C. Y.; Hanzlicek, J.; Cheng, S. Z. D.; Geil, P. H.; Grebowicz, J.; Ho, R. M. *Polymer* **2001**, *42*, 7171.
(37) Keith, H. D.; Chen, W. Y. *Polymer* **2002**, *43*, 6263.
(38) Polanyi, M. *Z. Phys.* **1921**, *7*, 149.
(39) Striebeck, N.; Nöchel, U. *J. Appl. Crystallogr.* **2009**, *42*, 295.